

RECEIVED: April 17, 2024

REVISED: March 22, 2025

ACCEPTED: May 21, 2025

PUBLISHED: June 18, 2025

Constraints on the X_{17} boson from IceCube searches for non-standard interactions of neutrinos

Rikard Enberg ^a, Yaşar Hiçyılmaz ^{b,c}, Stefano Moretti ^{a,c},
Carlos Pérez de los Heros ^a and Harri Waltari ^a

^aDepartment of Physics & Astronomy, Uppsala University,
Box 516, SE-751 20 Uppsala, Sweden

^bDepartment of Physics, Balıkesir University,
TR10145, Balıkesir, Turkey

^cSchool of Physics and Astronomy, University of Southampton,
Highfield, Southampton SO17 1BJ, U.K.

E-mail: rikard.enberg@physics.uu.se, yasarhicilyilmaz@balikesir.edu.tr,
stefano.moretti@physics.uu.se, cph@physics.uu.se,
harri.waltari@physics.uu.se

ABSTRACT: We explain the ATOMKI anomaly with a very light Z' state that features non-anomalous and non-flavour-universal vector and axial-vector couplings to all leptons. This Z' comes from a theoretical framework with a spontaneously broken $U(1)'$ symmetry in addition to the Standard Model gauge group and is compliant with current measurements of the anomalous magnetic moments of the electron and the muon as well as beam dump experiments. The lepton flavour structure of this model allows for Z' couplings to all light neutrinos, suggesting the possibility of Z' -mediated Non-Standard Interactions (NSIs) of neutrinos in matter, so that measurements of the strength parameters of the NSIs can constrain the value of the couplings. We use experimental constraints on NSIs of neutrinos using older TEXONO data and newer IceCube data. The IceCube data, in particular, strongly constrain the flavour universality of the leptonic vector current. The constraints enable us to define the region of parameter space of this theoretical scenario that can be pursued in further phenomenological analyses.

KEYWORDS: Multi-Higgs Models, New Light Particles, Specific BSM Phenomenology

ARXIV EPRINT: [2404.04717](https://arxiv.org/abs/2404.04717)

Contents

1	Introduction	1
2	The $U(1)'$ model	2
3	Neutrino NSIs	7
4	Constraints on NSIs from IceCube	9
5	Constraints on the $U(1)'$ model from other experiments	9
6	Results	10
7	Conclusions	13

1 Introduction

The discovery of the Higgs boson [1, 2] provided strong evidence that the Standard Model (SM) of particle physics is indeed a consistent, and successful, description of elementary particles and their interactions, at least at the energies probed so far in accelerators. There are, however, several experimental “anomalies” that could point to new physics Beyond the SM (BSM). The majority of the experimental results that cannot be explained within the SM have been uncovered in non-LHC experiments, such as $(g-2)_\mu$, the measured value of the magnetic moment of muon in the Muon $g-2$ experiment at Brookhaven National Laboratory (BNL) [3]. Another anomaly is the significant enhancement of more than 5σ in the invariant mass and angular distributions of electron-positron final states of decays of excited ^8Be measured by the ATOMKI collaboration in 2015 [4]. Most studies trying to understand this result have demonstrated that standard nuclear physics or QCD cannot lead to a satisfactory explanation [5–9]. The ATOMKI results can be accounted for by the existence of a new vector or axial-vector mediator with a mass of around 17 MeV, which has been called the $X17$ boson [10–18]. Further studies [19, 20] demonstrated that, due to conflicts with the non-observation of deviations from the SM in neutrino scattering experiments, the scenarios including a pure vector mediator are less favourable, while an axial-vector state appears as the most promising candidate to simultaneously explain all the anomalous nuclear decays reported by the ATOMKI collaboration [5]. In the case of a pure vector boson, the couplings of new boson to nucleons are strongly constrained by the NA48/2 experiment [21]. Moreover, the pure vector boson explanations could be ruled out under the strong experimental limits on pion decays [22], such as SINDRUM [23].

As a minimal approach, a family-dependent $U(1)'$ extension of the SM would be an ideal way to allow axial-vector couplings that could explain the ATOMKI anomaly while the vector couplings are also present. In this framework, the Yukawa interactions are modified by higher-dimensional operators [24, 25]. This scenario, which introduces a new light vector boson, Z' , also leads to Non-Standard Interactions (NSIs) of neutrinos that affect neutrino flavour ratios in matter [26]. Currently, limits from the TEXONO experiment have been derived on the combination $\sqrt{\epsilon_e \epsilon_\nu}$, where ϵ_e and ϵ_ν are the couplings of the Z' to electrons and

neutrinos, respectively. The limits imply that $\sqrt{\epsilon_e \epsilon_\nu} < 7 \times 10^{-5}$ for constructive interference and $\sqrt{\epsilon_e \epsilon_\nu} < 3 \times 10^{-4}$ for destructive interference [11, 27, 28]. Moreover, the experimental constraints on NSIs from neutrino oscillations can be applied to restrict the couplings of the new boson with SM fermions. For instance, in ref. [29], the authors presented the experimental NSI constraints on lepton flavour violating couplings for a Z' boson with a mass heavier than the τ lepton. In this paper, we will confront the ATOMKI anomaly and the anomalous magnetic moments of leptons with the NSI constraints reported by the IceCube collaboration [30]. We will show the allowed regions of couplings and the amount of non-universality in the minimal $U(1)'$ extension of the SM which satisfy IceCube constraints.

The rest of the paper is organised as follows. In section 2 we provide a brief discussion of the main components of the model. We discuss the general formalism of NSI dynamics in section 3 and the new constraints from IceCube that we use in our analysis in section 4. After summarising our computational procedure and enforcing experimental constraints in section 5, we present our results over the surviving parameter space of couplings and NSI parameters in section 6. Finally, we summarise and conclude in section 7.

2 The $U(1)'$ model

We focus on an extension of the SM with a generic $U(1)'$ symmetry which mixes with the SM $U(1)_Y$. The kinetic term of the Lagrangian is given by

$$\mathcal{L}_{\text{Kin}}^{U(1)'} = -\frac{1}{4} \hat{F}_{\mu\nu} \hat{F}^{\mu\nu} - \frac{1}{4} \hat{F}'_{\mu\nu} \hat{F}'^{\mu\nu} - \frac{\eta}{2} \hat{F}'_{\mu\nu} \hat{F}^{\mu\nu}, \quad (2.1)$$

where $F_{\mu\nu}$ and $F'_{\mu\nu}$ are the field strengths of the gauge fields B_μ and B'_μ that correspond to $U(1)_Y$ and $U(1)'$, respectively, and η quantifies the kinetic mixing between these abelian symmetries. The Lagrangian for the gauge sector can be diagonalised via a $GL(2, \mathbb{R})$ transformation which rescales the gauge fields as

$$\begin{pmatrix} \hat{B}_\mu \\ \hat{B}'_\mu \end{pmatrix} = \begin{pmatrix} 1 & -\frac{\eta}{\sqrt{1-\eta^2}} \\ 0 & \frac{1}{\sqrt{1-\eta^2}} \end{pmatrix} \begin{pmatrix} B_\mu \\ B'_\mu \end{pmatrix}, \quad (2.2)$$

where \hat{B}_μ and \hat{B}'_μ are original $U(1)_Y$ and $U(1)'$ gauge fields with off-diagonal kinetic terms while B_μ and B'_μ do not possess such terms. After the transformation in eq. (2.2), the gauge covariant derivative can be written as

$$\mathcal{D}_\mu = \partial_\mu + \dots + i g_1 Y B_\mu + i(\tilde{g} Y + g' Q') B'_\mu, \quad (2.3)$$

where Y and g_1 are the hypercharge and its gauge coupling while Q' and g' in the additional term are the $U(1)'$ charge and its gauge coupling, respectively. In addition, \tilde{g} is the mixed gauge coupling between the two gauge groups. In eq. (2.3), we have introduced the g' and \tilde{g} in terms of original diagonal gauge couplings and the kinetic mixing parameter η as

$$g' \equiv \frac{g_{U(1)'}}{\sqrt{1-\eta^2}}, \quad \tilde{g} \equiv -\frac{\eta g_1}{\sqrt{1-\eta^2}}. \quad (2.4)$$

The scalar potential of the model is

$$V(H, \chi) = -\mu^2 |H|^2 + \lambda |H|^4 - \mu_\chi^2 |\chi|^2 + \lambda_\chi |\chi|^4 + \kappa |\chi|^2 |H|^2, \quad (2.5)$$

where H is the SM Higgs doublet and κ is the mixing parameter that connects the SM and

χ Higgs fields. Unlike the SM Higgs sector, there are two physical Higgs states with their acquired Vacuum Expectation Values (VEVs)

$$\langle H \rangle = \frac{1}{\sqrt{2}} \begin{pmatrix} 0 \\ v \end{pmatrix}, \quad \langle \chi \rangle = \frac{v'}{\sqrt{2}}. \quad (2.6)$$

After Spontaneous Symmetry Breaking (SSB), the relation of the two CP-even mass eigenstates h_1 and h_2 with these physical states via an orthogonal transformation through a mixing matrix can be written as

$$\begin{pmatrix} h_1 \\ h_2 \end{pmatrix} = \begin{pmatrix} \cos \theta & -\sin \theta \\ \sin \theta & \cos \theta \end{pmatrix} \begin{pmatrix} H \\ \chi \end{pmatrix}, \quad (2.7)$$

where the mixing angle θ varies over the interval $-\pi/2 < \theta < \pi/2$. The mass eigenstates are

$$m_{h_{1,2}}^2 = \lambda v^2 + \lambda \chi v'^2 \mp \sqrt{(\lambda v^2 - \lambda \chi v'^2)^2 + (\kappa v v')^2}, \quad (2.8)$$

from where, using the physical masses $m_{h_{1,2}}$, the two VEVs v, v' and with the initial conditions of scalar couplings, one can get the following relation for the mixing angle [31]

$$\tan 2\theta = \frac{\kappa v v'}{\lambda v^2 - \lambda \chi v'^2}. \quad (2.9)$$

In this work, we assume that h_2 is dominantly the SM-like Higgs boson while the exotic boson h_1 is dominantly a singlet-like Higgs state. In ref. [32], the possible Z' signatures mediated by such Higgs bosons were worked out.

The $U(1)'$ symmetry is broken by a new scalar χ , which is a singlet under the SM gauge group and has $U(1)'$ charge Q'_χ and its VEV shown in eq. (2.6). The spontaneous breaking of the $U(1)'$ symmetry results in the mass term of a new vector boson. The mass eigenstates of the neutral gauge bosons are obtained by the transformation as

$$\begin{pmatrix} B^\mu \\ W_3^\mu \\ B'^\mu \end{pmatrix} = \begin{pmatrix} \cos \theta_W & -\sin \theta_W \cos \theta' & \sin \theta_W \sin \theta' \\ \sin \theta_W & \cos \theta_W \cos \theta' & -\cos \theta_W \sin \theta' \\ 0 & \sin \theta' & \cos \theta' \end{pmatrix} \begin{pmatrix} A^\mu \\ Z^\mu \\ Z'^\mu \end{pmatrix}, \quad (2.10)$$

where θ_W is the usual Weinberg angle and θ' is $Z - Z'$ mixing angle defined as [31]

$$\tan 2\theta' = \frac{2g_H \sqrt{g_2^2 + g_1^2}}{g_H^2 + (2Q'_\chi g' v'/v)^2 - g_2^2 - g_1^2}, \quad (2.11)$$

where $g_H = \tilde{g} + 2g'Q'_H$. The mixing angle θ' is strictly constrained by the bounds from the precision tests in the LEP experiment as $|\theta'| \lesssim 10^{-3}$ [33, 34]. In the case of small θ' , the gauge boson masses can be read in terms of $m_{Z,Z'}$ as

$$m_Z \simeq \frac{v}{2} \sqrt{g_2^2 + g_1^2}, \quad m_{Z'} \simeq \frac{v}{2} \sqrt{g_H^2 + (2Q'_\chi g' v'/v)^2}, \quad (2.12)$$

while θ' is rewritten as

$$\theta' \simeq g_H \frac{m_Z^2}{m_{Z'}^2 - m_Z^2}. \quad (2.13)$$

In the case of $g' \sim \mathcal{O}(10^{-4} - 10^{-5})$, $M_{Z'}$ would be light, with a mass of $\mathcal{O}(10)$ MeV, which is the desired mass region for a potential solution of the ATOMKI anomaly if v' is of order $\mathcal{O}(100 - 1000)$ GeV.

The Lagrangian that describes the interactions of the extra gauge boson Z' with SM fermions is

$$\begin{aligned} \mathcal{L}^{Z'} = & \bar{q}\gamma^\mu \left(C_L^{qq'} P_L + C_R^{qq'} P_R \right) q' Z'_\mu + \bar{\nu}_l \gamma^\mu \left(C_L^{ll'} P_L \right) \nu_{l'} Z'_\mu \\ & + \bar{l}\gamma^\mu \left(C_L^{ll'} P_L + C_R^{ll'} P_R \right) l' Z'_\mu, \end{aligned} \quad (2.14)$$

where $q^{(l)}$, $l^{(l)}$ and $\nu_{l^{(l)}}$ refer to up-type/down-type quarks, charged leptons and their neutrinos while C_L^{XX} and C_R^{XX} are Left (L) and Right (R) handed couplings and P_L and P_R the corresponding projection operators $\frac{1 \mp \gamma^5}{2}$, respectively. In our model, there are no flavour-violating (non-diagonal) coupling terms for the quark and lepton sector while the flavour-conserving (diagonal) $f = f'$ coupling terms are written as

$$C_L^{ff} = -g_Z \sin \theta' \left(T_f^3 - \sin^2 \theta_W Q_f \right) + (\tilde{g} Y_{f,L} + g' Q'_{f,L}) \cos \theta', \quad (2.15)$$

$$C_R^{ff} = g_Z \sin^2(\theta_W) \sin(\theta') Q_f + (\tilde{g} Y_{f,R} + g' Q'_{f,R}) \cos \theta', \quad (2.16)$$

where $g_Z = \sqrt{g_1^2 + g_2^2}$ is the Electro-Weak (EW) coupling. Here, T_f^3 and Q_f denote the weak isospin and electric charge of the fermion f , respectively. Finally, $Y_{f,L/R}$ and $Q'_{f,L/R}$ indicate the hypercharge and $U(1)'$ charges of the L/R -handed fermion.

Considering the interactions in eq. (2.14), the Z' boson undoubtedly contributes to the Anomalous Magnetic Moments (AMMs) of the charged leptons a_f , for $f = e, \mu, \tau$. Such contributions could be determined by their vector and axial couplings and the mass of the Z' boson $m_{Z'}$ as [35]

$$\begin{aligned} \Delta a_f = & \frac{m_f^2}{4\pi^2 m_{Z'}^2} \left(C_{f,V}^2 \int_0^1 \frac{x^2(1-x)}{1-x+x^2 m_\alpha^2/m_{Z'}^2} dx \right. \\ & \left. - C_{f,A}^2 \int_0^1 \frac{x(1-x)(4-x) + 2x^3 m_f^2/m_{Z'}^2}{1-x+x^2 m_f^2/m_{Z'}^2} dx \right), \end{aligned} \quad (2.17)$$

where the vector and axial couplings defined by eqs. (2.15) and (2.16) as

$$C_{f,V} = \frac{C_R^{ff} + C_L^{ff}}{2}, \quad C_{f,A} = \frac{C_R^{ff} - C_L^{ff}}{2}. \quad (2.18)$$

In the limit of small gauge coupling and mixing, $g', \tilde{g} \ll 1$, we can redefine the vector and axial couplings as [16]

$$\begin{aligned} C_{f,V} & \cong \tilde{g} \cos^2(\theta_W) Q_f + g' [Q'_H (T_f^3 - 2 \sin^2(\theta_W) Q_f) + (Q'_{f,R} + Q'_{f,L})/2], \\ C_{f,A} & \cong g' [-Q'_H T_f^3 + (Q'_{f,R} - Q'_{f,L})/2]. \end{aligned} \quad (2.19)$$

For the limits $m_f \ll m_{Z'}$ and $m_f \gg m_{Z'}$, eq. (2.17) reduces to [36]

$$\Delta a_f \simeq \begin{cases} m_f^2 \left(C_{f,V}^2 - 5C_{f,A}^2 \right) / (12\pi^2 m_{Z'}^2), & m_f \ll m_{Z'}, \\ (m_{Z'}^2 C_{f,V}^2 - 2m_f^2 C_{f,A}^2) / (8\pi^2 m_{Z'}^2), & m_f \gg m_{Z'}. \end{cases} \quad (2.20)$$

For $M_{Z'} \simeq 17 \text{ MeV}$, one then finds

$$\Delta a_e = 7.6 \times 10^{-6} C_{e,V}^2 - 3.8 \times 10^{-5} C_{e,A}^2, \quad (2.21)$$

$$\Delta a_\mu = 0.009 C_{\mu,V}^2 - C_{\mu,A}^2. \quad (2.22)$$

The contribution from Z' to $B_s \rightarrow \mu^+ \mu^-$ can be parameterised as [37]

$$BR(B_s \rightarrow \mu^+ \mu^-) = \frac{|V_{tb} V_{ts}^*|^2 G_F^2}{16\pi^3} m_{B_s} m_\mu^2 \alpha^2 \tau_{B_s} f_{B_s}^2 \sqrt{1 - \frac{4m_\mu^2}{m_{B_s}^2}} (C_{10\mu} - C_{10'\mu})^2. \quad (2.23)$$

For detailed information about Z' contribution to other rare B decays, please see in ref. [38].

Furthermore, one of the new physics effect of the Z' boson is manifest in neutrino scattering experiments in the presence of non-zero neutrino couplings in eq. (2.14). If we consider the TEXONO experiment, which probes neutrino-electron scatterings as mentioned in section 1, the correction to the SM cross-section of anti-neutrino scattering for $m_{Z'} \gtrsim 10 \text{ MeV}$ in terms of the Z' -electron couplings is [36, 39]

$$\begin{aligned} \frac{\sigma(\bar{\nu}_e e^- \rightarrow \bar{\nu}_e e^-)}{\sigma(\bar{\nu}_e e^- \rightarrow \bar{\nu}_e e^-)^{\text{SM}}} &\simeq 1 + (2.07 C_{e,V} + 1.39 C_{e,A}) 10^{11} C_L^{\nu_e \nu_e} \left(\frac{\text{MeV}}{m_{Z'}}\right)^2 \\ &+ \left(1.37 C_{e,V}^2 + 2.62 C_{e,V} C_{e,A} + 1.64 C_{e,A}^2\right) \left(10^{11} C_L^{\nu_e \nu_e}\right)^2 \left(\frac{\text{MeV}}{m_{Z'}}\right)^4. \end{aligned} \quad (2.24)$$

It is easy to note that AMM and neutrino scattering experiments put additional bounds on Z' -fermion couplings as well as neutrino oscillation experiments such as IceCube via NSI effective couplings.

Let us now consider the Yukawa sector of our model. The Yukawa Lagrangian of the SM is

$$-\mathcal{L}_{\text{Yuk.}}^{\text{SM}} = Y_u \bar{Q} \tilde{H} u_R + Y_d \bar{Q} H d_R + Y_e \bar{L} H e_R. \quad (2.25)$$

In order to satisfy gauge invariance, the charges of the fields under the $U(1)'$ group must obey the condition of

$$-Q'_Q - Q'_H + Q'_u = -Q'_Q + Q'_H + Q'_d = -Q'_L + Q'_H + Q'_e = 0. \quad (2.26)$$

Considering eqs. (2.15) and (2.16) with these relations, one can find no axial-vector couplings to the Z' for quarks and leptons. In this work, our theoretical model relies on flavour-dependent charges of the Z' . Having such non-universal $U(1)'$ charges allows axial-vector couplings of the Z' with nucleons, which are crucial to overcome the strict experimental bounds in the pure vector coupling case [10, 11, 21]. To achieve this, a new mechanism is identified that generates masses and couplings of the first two fermion generations at higher orders as the SM-like Yukawa interactions are available only for the third generation. In this case, the Yukawa interaction terms for first two fermion families are modified as

$$\begin{aligned} -\mathcal{L}_{\text{Yuk.}} &= \Gamma^u \frac{\chi^{n_{ij}}}{M^{n_{ij}}} \bar{Q}_{L,i} \tilde{H} u_{R,j} + \Gamma^d \frac{\chi^{l_{ij}}}{M^{l_{ij}}} \bar{Q}_{L,i} H d_{R,j} \\ &+ \Gamma^e \frac{\chi^{m_{ij}}}{M^{m_{ij}}} \bar{L}_i H e_{R,j} + h.c., \end{aligned} \quad (2.27)$$

where M is the non-renormalisable scale whose dimension is determined by the $U(1)'$ charges of the involved fields [25]. Here, we are able to obtain axial-vector couplings for the first two generations of quarks to successfully reproduce the ATOMKI anomaly,

$$\begin{aligned} -Q'_{Q_{1,2}} - Q'_H + Q'_{u_{1,2}} &\neq 0 \\ -Q'_{Q_{1,2}} + Q'_H + Q'_{d_{1,2}} &\neq 0. \end{aligned} \tag{2.28}$$

The charges must also satisfy the anomaly cancellation conditions for the fermionic content of the SM and the additional R -handed neutrinos:

$$\sum_{i=1}^3 (2Q'_{Q_i} - Q'_{u_i} - Q'_{d_i}) = 0, \tag{2.29}$$

$$\sum_{i=1}^3 (3Q'_{Q_i} + Q'_{L_i}) = 0, \tag{2.30}$$

$$\sum_{i=1}^3 \left(\frac{Q'_{Q_i}}{6} - \frac{4}{3}Q'_{u_i} - \frac{Q'_{d_i}}{3} + \frac{Q'_{L_i}}{2} - Q'_{e_i} \right) = 0, \tag{2.31}$$

$$\sum_{i=1}^3 (Q'^2_{Q_i} - 2Q'^2_{u_i} + Q'^2_{d_i} - Q'^2_{L_i} + Q'^2_{e_i}) = 0, \tag{2.32}$$

$$\sum_{i=1}^3 (6Q'^3_{Q_i} - 3Q'^3_{u_i} - 3Q'^3_{d_i} + 2Q'^3_{L_i} - Q'^3_{e_i}) + \sum_{i=1}^3 Q'^3_{\nu_i} = 0, \tag{2.33}$$

$$\sum_{i=1}^3 (6Q'_{Q_i} - 3Q'_{u_i} - 3Q'_{d_i} + 2Q'_{L_i} - Q'_{e_i}) + \sum_{i=1}^3 Q'_{\nu_i} = 0. \tag{2.34}$$

In addition to these conditions, we also impose that the first two generations of quarks are flavour-universal under $U(1)'$ in order to alleviate experimental bounds on flavour violating interactions of quarks, i.e., $Q'_{Q_1} = Q'_{Q_2}, Q'_{d_1} = Q'_{d_2}, Q'_{u_1} = Q'_{u_2}$. Conversely, for the purpose of this study, the $U(1)'$ charges of the lepton sector were left as fully non-universal. We can then express the fifteen charges in terms of the four charges $Q'_{L_1}, Q'_{Q_1}, Q'_{Q_3}, Q'_{\nu_1}$ that are free model parameters, by using the conditions

$$\begin{aligned} Q'_{L_1} + Q'_{L_2} + 6Q'_{Q_1} &= 0, \\ Q'_{L_3} + 3Q'_{Q_3} &= 0, \\ Q'_{d_1} + 2Q'_{Q_1} &= 0, \\ Q'_{d_3} + 2Q'_{Q_1} &= 0, \\ Q'_{u_1} - 4Q'_{Q_1} &= 0, \\ Q'_{u_3} - 2Q'_{Q_1} - 2Q'_{Q_3} &= 0, \\ Q'_{e_1} + Q'_{L_1} + 9Q'_{Q_1} &= 0, \\ Q'_{e_2} - Q'_{L_1} + 3Q'_{Q_1} &= 0, \\ Q'_{e_3} + 4Q'_{Q_3} + 2Q'_{Q_1} &= 0, \\ Q'_{\nu_1} + Q'_{\nu_2} &= 0, \\ Q'_{\nu_3} - 2Q'_{Q_3} + 2Q'_{Q_1} &= 0, \\ Q'_H - 2Q'_{Q_1} - Q'_{Q_3} &= 0. \end{aligned} \tag{2.35}$$

The relations in eq. (2.35) are derived from eqs. (2.29)–(2.34) and from the Yukawa conditions for only the third fermion family in eq. (2.26), and allow us to find numerical solutions satisfying the anomaly cancellation equations exactly. We scan numerically over integer solutions for the free charges, for absolute values from 1 to $Q_{\max} = 200$. Larger Q_{\max} is possible, but since the number of solutions grows rapidly with Q_{\max} , this can lead to numerical problems. We then normalise all integer solutions by dividing by 100, thus obtaining rational solutions with the absolute free charges $|Q'| < 2$.

In the next section, we present the general formalism for NSIs and how these non-universal charges relate to the NSI parameters.

3 Neutrino NSIs

New physics effects in the neutrino sector, such as couplings between neutrinos and unknown particles, can be described by a model independent four-fermion effective Lagrangian that corresponds to NSIs [40, 41]. The NSI Lagrangian including Neutral Currents (NCs) can be parameterised in terms of the dimensionless NSI parameters $\varepsilon_{\alpha\beta}^{fX}$ as

$$\mathcal{L}_{\text{NSI}}^{\text{NC}} = -2\sqrt{2}G_F\varepsilon_{\alpha\beta}^{fX}[\bar{f}\gamma^\mu P_X f][\bar{\nu}_\alpha\gamma_\mu P_L\nu_\beta], \quad (3.1)$$

where X is either L or R , $f = u, d, e$ and G_F is the Fermi constant. Neutrino flavours are given by $\alpha, \beta = e, \mu, \tau$. In the case of $\alpha \neq \beta$, the NSI parameters imply flavour-violating new physics interactions in eq. (3.1), while $\alpha = \beta$ indicates flavour-conserving NSI terms. The former lead to zero-distance flavour-changing effects, which one can probe with the near detector of oscillation experiments. Both flavour-conserving and flavour-violating effects can lead to a modification of matter oscillations [42, 43] to which IceCube is sensitive. Since gauge interactions are (nearly) flavour-diagonal, we concentrate on flavour-conserving interactions in what follows.

Considering the effective Lagrangian in eq. (3.1), we have a relation between the NSI parameters and the propagator of the mediator, $\varepsilon_{\alpha\beta}^{fX} \propto \frac{1}{q^2 - M^2}$, where q and M are the mediator momentum and mass, respectively. Matter oscillations arise from the interference of unperturbed propagation and gauge boson exchange in the forward direction, thus the limit $q^2 \rightarrow 0$ applies, so that the mass term dominates in the denominator even if the gauge boson is light. Therefore, an additional Z' boson which satisfies the ATOMKI anomaly could provide a non-trivial contribution to the matter NSI parameters. Using the interaction terms in eq. (2.14), it is possible to generate the Z' -mediated effective NSI Lagrangian in eq. (3.1), with corresponding NSI parameters

$$\varepsilon_{\alpha\beta}^{fX} = \frac{1}{2\sqrt{2}G_F} \frac{C_L^{\alpha\beta} C_X^{ff}}{M_{Z'}^2}. \quad (3.2)$$

The $\varepsilon_{\alpha\beta}^{fX}$ are the effective couplings of neutrinos with fundamental fermions and affect neutrino propagation in matter. The relevant NSI effective couplings for neutrino propagation in a medium are their vector parts, $\varepsilon_{\alpha\beta}^{fV} = \varepsilon_{\alpha\beta}^{fL} + \varepsilon_{\alpha\beta}^{fR}$, and the total strength of NSIs for a given medium has the form

$$\epsilon_{\alpha\beta} = \sum_f (\varepsilon_{\alpha\beta}^{fV}) \frac{N_f}{N_e}, \quad (3.3)$$

where $f = u, d, e$. Here N_f is the number density of the fermion f in matter. Inside the Sun, $N_u/N_e \simeq 2N_d/N_e \simeq 1$ [44] while inside the Earth, $N_u/N_e \simeq N_d/N_e \simeq 3$ [45]. Notice that the axial vector part of the current does not contribute and hence matter oscillations will not constrain it. In the presence of NSI couplings of neutrinos with the matter field f , the effective Hamiltonian is written as

$$H = \frac{1}{2E_\nu} U_{\text{PMNS}} \text{diag}(0, \Delta m_{21}^2, \Delta m_{31}^2) U_{\text{PMNS}}^\dagger + V_{\text{CC}} \text{diag}(1, 0, 0) + V_{\text{CC}} \epsilon_{\alpha\beta}, \quad (3.4)$$

where U_{PMNS} is the vacuum Pontecorvo-Maki-Nakagawa-Sakata (PMNS) matrix while E_ν and $\Delta m_{ij}^2 \equiv \Delta m_i^2 - \Delta m_j^2$ are the neutrino energy and mass square differences, respectively. The second term describes the SM interactions in an unpolarised medium with the Wolfenstein matter potential $V_{\text{CC}} = \sqrt{2}G_F N_e$ [42], where N_e is the local electron number density. The last term of eq. (3.4) is the NSI contribution, where the Hermitian matrix of the NSI strength parameters $\epsilon_{\alpha\beta}$ shown in eq. (3.3) can be written as

$$\epsilon_{\alpha\beta} = \begin{pmatrix} \epsilon_{ee} & \epsilon_{e\mu} & \epsilon_{e\tau} \\ \epsilon_{e\mu}^* & \epsilon_{\mu\mu} & \epsilon_{\mu\tau} \\ \epsilon_{e\tau}^* & \epsilon_{\mu\tau}^* & \epsilon_{\tau\tau} \end{pmatrix}. \quad (3.5)$$

The diagonal terms in eq. (3.5), if non-universal, lead to enhanced matter oscillations proportional to the difference in the diagonal NSI parameters, i.e., to $\epsilon_{\tau\tau} - \epsilon_{\mu\mu}$ and $\epsilon_{ee} - \epsilon_{\mu\mu}$. Since any flavour-universal part gives just an unobservable common phase to the neutrinos, one can subtract $\epsilon_{\mu\mu}$ from the diagonal in eq. (3.5), then the diagonal part of the matrix $\epsilon_{\alpha\beta}$ can be written as $\text{diag}(\epsilon_{ee} - \epsilon_{\mu\mu}, 0, \epsilon_{\tau\tau} - \epsilon_{\mu\mu})$.

We approximate the hadrons to consist of their valence quarks,¹ so we write the NSI parameters of the effective matter potential in terms of electron, proton and neutron NSI parameters as

$$\epsilon_{\alpha\beta}^\oplus = \epsilon_{\alpha\beta}^{eV} + \epsilon_{\alpha\beta}^{pV} + Y_n^\oplus \epsilon_{\alpha\beta}^{nV}, \quad (3.6)$$

where $\epsilon_{\alpha\beta}^{pV} = 2\epsilon_{\alpha\beta}^{uV} + \epsilon_{\alpha\beta}^{dV}$, $\epsilon_{\alpha\beta}^{nV} = 2\epsilon_{\alpha\beta}^{dV} + \epsilon_{\alpha\beta}^{uV}$ and Y_n^\oplus is the relative neutron-to-electron number density of the Earth, $Y_n^\oplus \equiv N_n/N_e \approx 1.051$ [46]. Finally, one can obtain the NSI matrix in the Hamiltonian with new definitions as

$$\epsilon_{\alpha\beta}^\oplus = \begin{pmatrix} \epsilon_{ee}^\oplus - \epsilon_{\mu\mu}^\oplus & \epsilon_{e\mu}^\oplus & \epsilon_{e\tau}^\oplus \\ \epsilon_{e\mu}^{\oplus*} & 0 & \epsilon_{\mu\tau}^\oplus \\ \epsilon_{e\tau}^{\oplus*} & \epsilon_{\mu\tau}^{\oplus*} & \epsilon_{\tau\tau}^\oplus - \epsilon_{\mu\mu}^\oplus \end{pmatrix}. \quad (3.7)$$

Notice again that there is no flavour violation (non-diagonal terms) in the theoretical model of this work.

¹The Z' , being uncoloured, does not see the gluonic sea. Since the momentum transfer is low, it cannot resolve the internal structure of the proton. Hence quark-antiquark pairs, having opposite charges (being dipole-like objects), will to first approximation look neutral and only the monopole charges of the valence quarks will be seen by the Z' boson.

Parameter	Scanned range	Parameter	Scanned range
g'	$[10^{-5}, 5 \times 10^{-5}]$	λ	$[0.125, 0.132]$
\tilde{g}	$[-10^{-3}, 10^{-3}]$	λ_χ	$[10^{-5}, 10^{-1}]$
v'	$[0.1, 1]$ TeV	κ	$[10^{-6}, 10^{-2}]$
$Q'_{Q_1}, Q'_{Q_3}, Q'_{L_1}$	$[-2, 2]$	Q'_{ν_1}	0

Table 1. Scanned parameter space of the model.

4 Constraints on NSIs from IceCube

The previous generic parameterisation of the strength of NSIs as shown in eq. (3.7) has been used by the IceCube collaboration in ref. [30] to constrain the parameters $\epsilon_{ee}^\oplus - \epsilon_{\mu\mu}^\oplus$, $\epsilon_{\tau\tau}^\oplus - \epsilon_{\mu\mu}^\oplus$, $|\epsilon_{e\mu}^\oplus|$, $|\epsilon_{e\tau}^\oplus|$ and $|\epsilon_{\mu\tau}^\oplus|$ using a pure sample of atmospheric neutrinos (and antineutrinos) of all flavours with energies between 5.6 GeV and 100 GeV. The use of atmospheric neutrinos allows to sample a wide range of oscillation baselines, from a few tens of kilometres, for downgoing neutrinos produced “above” the detector that only cross the atmosphere, to the whole diameter of the Earth, 1.3×10^4 km, for upgoing neutrinos produced at the antipodes of the detector. Matter effects can thus be expected for neutrinos arriving to the detector from below the horizon, while the atmosphere is too thin to induce any matter effects on the neutrino flux arriving to the detector from above.

Comparing the measured flavour composition of the neutrino flux at the detector as a function of energy and baseline with the expected corresponding flux under standard oscillations, strong limits on the NSI parameters can be set. Note that these constraints were obtained by allowing one of the parameters to be non-zero at a time. We do not consider flavour-violating terms in our study, so we only use the IceCube limits on flavour-diagonal interactions, shown in table 2, in order to put constraints on the model described in section 2.

5 Constraints on the U(1)' model from other experiments

To define the parameter space of our model we have used the SPheno [47–49] and SARAH 4.14.3 [50, 51] codes. The scanning of the parameter space was performed using the Metropolis-Hastings algorithm, within the ranges specified in table 1.

Before applying the NSI constraints from IceCube [30] to our U(1)' model, some important experimental outcomes have been implemented to our results from the parameter space scan. We first require the Higgs boson mass to be within 3 GeV of its observed value of 125 GeV and implement constraints on the Branching Ratios (BRs) of rare B -decays, specifically $\text{BR}(B \rightarrow X_s \gamma)$, $\text{BR}(B_s \rightarrow \mu^+ \mu^-)$ and $\text{BR}(B_u \rightarrow \tau \nu_\tau)$ [52–54]. We have also bounded the value of the $Z - Z'$ mixing parameter θ' (see eq. (2.11)) to be less than a few times 10^{-3} as a result of EW Precision Tests (EWPTs) [33, 34].

In the following part of the numerical analyses, we constrain the parameter space to satisfy the current experimental bounds on AMM results for $(g - 2)_e$, $(g - 2)_\mu$ [55, 56], the ATOMKI anomaly [19], the electron beam dump experiment NA64 [57], which probes the Z' couplings to electrons, $C_{e,V}^2 + C_{e,A}^2$, in any possible production and detection via $e^- + Z \rightarrow e^- + Z' [\rightarrow e^+ e^-]$ and neutrino scattering from the TEXONO experiment [27].

Observable	Constraint	Tolerance	Reference(s)
m_h	122 GeV – 128 GeV		
$\text{BR}(B_s \rightarrow \mu^+ \mu^-)$	$0.8 \times 10^{-9} - 6.2 \times 10^{-9}$	2σ	[53]
$\text{BR}(B \rightarrow X_s \gamma)$	$2.99 \times 10^{-4} - 3.87 \times 10^{-4}$	2σ	[52]
$\frac{\text{BR}(B_u \rightarrow \tau \nu_\tau)}{\text{BR}(B_u \rightarrow \tau \nu_\tau)_{\text{SM}}}$	0.15 – 2.41	3σ	[54]
Δa_e^{Rb}	$(4.8 \pm 9.0) \times 10^{-13}$	3σ	[56]
Δa_μ	$(2.45 \pm 1.47) \times 10^{-9}$	3σ	[55]
$\epsilon_{ee}^\oplus - \epsilon_{\mu\mu}^\oplus$	$[-2.26, -1.27] \cup [-0.74, 0.32]$		[30]
$\epsilon_{\tau\tau}^\oplus - \epsilon_{\mu\mu}^\oplus$	$[-0.041, 0.042]$		[30]
$\sqrt{C_{e,V}^2 + C_{e,A}^2}$	$\gtrsim 3.6 \times 10^{-5} \times \sqrt{\text{BR}(Z' \rightarrow e^+ e^-)}$		[57]
$\sqrt{C_{e,V} \times C_{\nu_e}}$	$\lesssim 3 \times 10^{-4}$		[27]
$ C_{e,V} \times C_{e,A} $	$\lesssim 10^{-8}$		[58, 59]
$ C_{e,A} \left \frac{188}{399} C_{u,V} + \frac{211}{399} C_{d,V} \right $	$\lesssim 1.8 \times 10^{-12}$		[60, 61]
$\sqrt{ C_n \times C_{\nu_e} }$	$\lesssim 13.6 \times 10^{-5}$		[20, 62–64]

Table 2. Summary of the experimental constraints used.

In the process of our Benchmark Point (BP) selection, we have also applied additional experimental limits on parity-violating Moller scattering [58, 59], atomic parity violation [60, 61] and Coherent Elastic neutrino-Nucleus Scattering (CEvNS) [20, 62–64] as $|C_{e,V} \times C_{e,A}| \lesssim 10^{-8}$, $|C_{e,A}| \left| \frac{188}{399} C_{u,V} + \frac{211}{399} C_{d,V} \right| \lesssim 1.8 \times 10^{-12}$ and $\sqrt{|C_n C_{\nu_e}|} \lesssim 13.6 \times 10^{-5}$, respectively. Here, C_n is the Z' -neutron coupling defined as $C_n = C_{u,V} + 2C_{d,V}$. The experimental constraints are summarised in table 2.

6 Results

In this section, we present the numerical analysis in the light of the experimental constraints from the previous section. First, let us focus on the diagonal NSI parameters shown in eq. (3.7). Figure 1 depicts the distribution of these parameters after scanning the parameter space. All points are consistent with Higgs mass bounds and the $Z - Z'$ mixing satisfying EWPTs. Green points are a subset of the grey ones as they also satisfy constraints on B -decays and Z' mass around 17 MeV. Yellow points are a subset of the green ones as they are also compatible with the current experimental bounds of $(g - 2)_\mu$ while blue points, that are a subset of the yellow ones, also satisfy the experimental limits from $(g - 2)_e$, NA64 and TEXONO. The red painted area represents the region allowed by IceCube results. As can be seen from the figure, most of our solutions are ruled out by the IceCube bounds on NSI parameters.

In the light of these strict bounds, we will show the constraints on Z' couplings. In figure 2, we represent the allowed vector and axial-vector Z' couplings with up-quarks (top left), down-quarks (top right) and electron (bottom). The colour convention is the same as in figure 1 while additional red points are a subset of the blue ones as they also satisfy the NSI

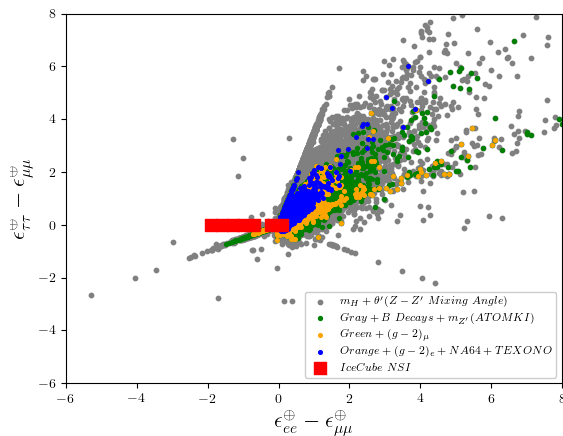


Figure 1. The distribution of diagonal NSI parameters shown in eq. (3.7). All points are consistent with Higgs mass bounds and the $Z - Z'$ mixing satisfying EWPTs. Green points are a subset of the grey ones as they also satisfy constraints on B -decays and Z' mass around 17 MeV. Yellow points are a subset of the green ones as they are also compatible with the current experimental bounds of $(g - 2)_\mu$ while blue points, that are a subset of the yellow ones, also satisfy the experimental limits from $(g - 2)_e$, NA64 and TEXONO. The red squares inside the blue points represent the region allowed by IceCube results in table 2.

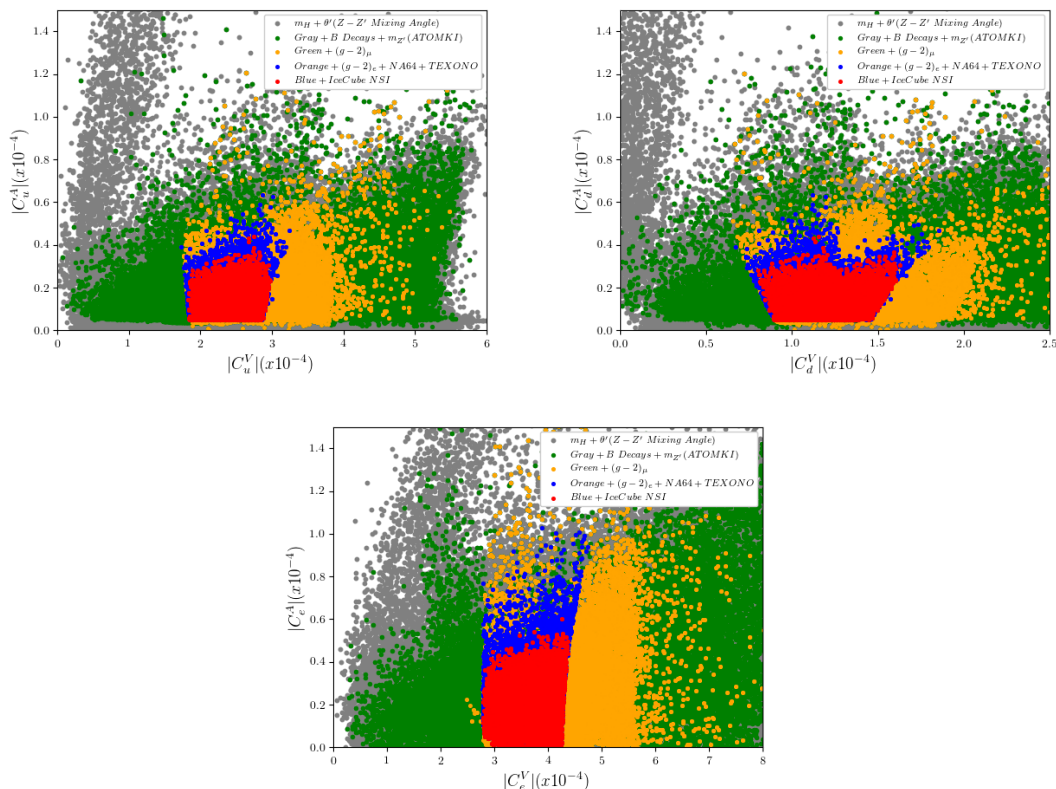


Figure 2. The allowed regions for the vector and axial-vector Z' couplings with up-quarks (top left), down-quarks (top right), electron (bottom). The colour convention is the same as in figure 1 while additional red points are a subset of the blue ones as they also satisfy the NSI parameters allowed by IceCube results.

parameters allowed by IceCube results. According to our results, the vector couplings between Z' and u, d, e , the fundamental particles in the medium, tend to be in the small interval of $\mathcal{O}(10^{-4})$ order while the axial-couplings should be at the order of $\mathcal{O}(10^{-5})$. Here, the vertical limitations on the couplings mainly arise from the experimental bound on the AMM of the electron in table 2 which is used for blue and then red points. As can be seen from eq. (2.21), $C_{e,V}$ has lower and upper limits for $C_{e,A} \simeq \mathcal{O}(10^{-5})$. These limits also impacts the couplings of the u and d quarks with Z' through the charge relations in eq. (2.35). Since the effective NSI couplings are related to the vector parts of the NSI parameters shown in eq. (3.3), the vector couplings are strongly bounded by IceCube constraints on NSIs.

Furthermore, figure 3 presents the distributions of electron neutrino (top left), muon neutrino (top right) and tau neutrino (bottom) in terms of their ratios to each other. As can be seen from the panels in the figure, when all constraints are applied, the Z' couplings with all neutrinos are restricted to be smaller than of $\mathcal{O}(5 \times 10^{-5})$. Since, in principle, the diagonal NSI terms in eq. (3.7) arise from the non-universality in the lepton sector, it is not hard to guess that the major impact of the IceCube results will be on non-universality of the Z' -lepton couplings. When we also look at the ratios of the Z' couplings with each neutrino flavour, it can be easily seen that the number of solutions for $|C_{\nu_\tau}/C_{\nu_\mu}|$ that satisfy IceCube constraints condense around 1. It means that those for μ and τ neutrinos should be universal, $|C_{\nu_\mu}/C_{\nu_\tau}| \approx 1$, because of the small values of $\epsilon_{\tau\tau}^\oplus - \epsilon_{\mu\mu}^\oplus$, according to the NSI bounds from IceCube. In contrast, the ratio for electron neutrino coupling such as $|C_{\nu_e}/C_{\nu_\mu}|$, can be seen as larger values in much more solutions, for the reason that the $\epsilon_{ee}^\oplus - \epsilon_{\mu\mu}^\oplus$ parameter gets looser bounds from IceCube data. There are also certain other discrete values of coupling ratios that seem to be preferred. These are cases, where the Higgs charge Q'_H is either exactly or close to zero (see eq. (2.35)). In that case the Higgs charge gives a smaller contribution to the mixing angle θ' (eq. (2.11)) than otherwise and hence there will be a lot more points that are acceptable based on the Z - Z' mixing.

Figure 4 indicates the allowed regions for the ratios of Z' vector (top) and axial-vector (bottom) couplings with e, μ and τ leptons. Here, the colour convention is the same as in figure 2. As we expected, the ratios of vector couplings are mostly bounded. It is important to note that, after applying the NSI constraints from IceCube as well, the vector couplings between Z' and charged leptons should be of the same magnitude, $|C_\tau^V/C_e^V| \approx |C_\tau^V/C_\mu^V| \approx 1$, that can be deemed universal, while the axial-vector Z' couplings for each charged lepton, not constrained by IceCube data, allow significant non-universality, as $0 < |C_e^A/C_\mu^A| < 30$ and $0 < |C_\tau^A/C_\mu^A| < 8$. Therefore, one can expect that possible signatures for such theoretical frameworks could be explored in Lepton Flavour Violation (LFV) processes which are more sensitive to the new boson axial couplings than its vector couplings.

Before closing, we investigate how the IceCube bounds impact the relevant NSI effective couplings for neutrino propagation. Figure 5 displays the allowed regions for NSI effective couplings of neutrinos with up-quarks (top), down-quarks (middle) and electrons (bottom) via Z' mediation. The colour convention is the same as in figure 2. As can be seen from the graphs, in the light of the IceCube results, all effective couplings are restricted to the region with $\epsilon \lesssim 10$. Considering the solutions which satisfy all experimental constraints except for NSI bounds (blue points), it is clear that the effective couplings, via light vector

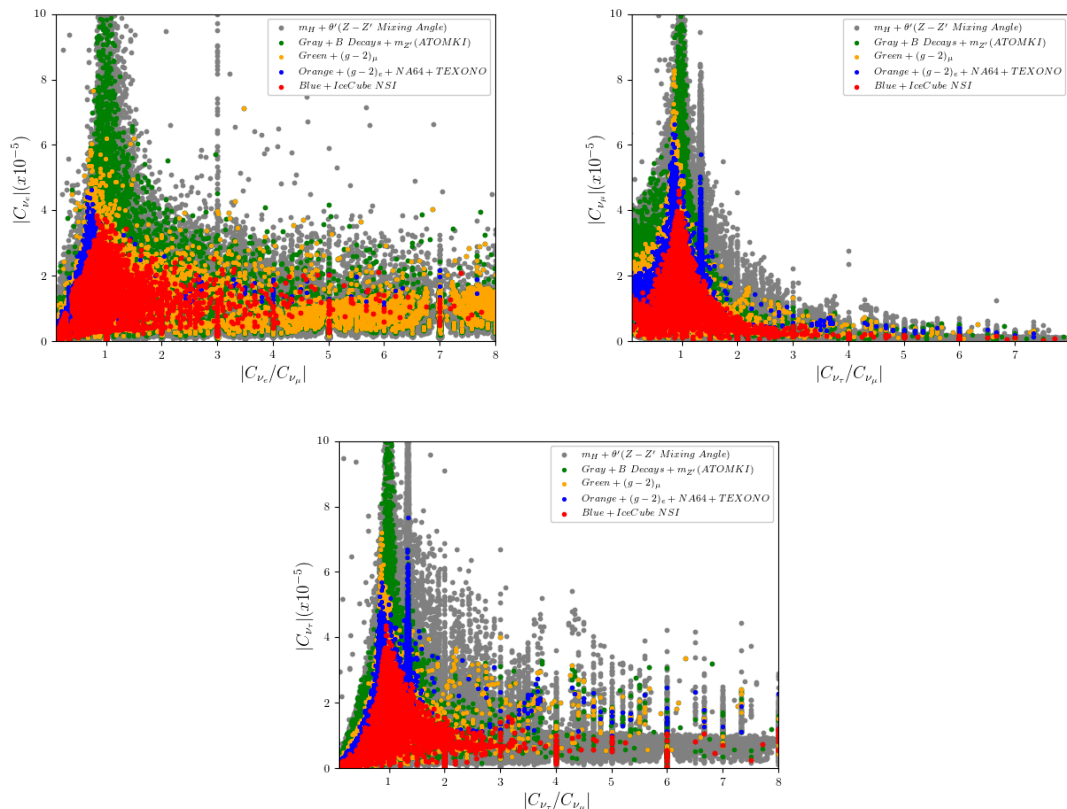


Figure 3. The allowed regions for the Z' couplings with ν_e, ν_μ (top) and ν_τ (bottom) versus their ratios to each other. Here, the colour convention is the same as in figure 2.

boson mediation between neutrinos and the components of the atoms in the medium, are limited by IceCube results.

To finalise our discussion about these results, we display four BPs: in fact, Table 3 displays four solutions which are selected to be consistent with all experimental constraints applied in our analyses as well as NSI results from IceCube.

7 Conclusions

We have described a rather simple theoretical framework that relies on a $U(1)'$ extension of the SM with non-anomalous and flavour-dependent charges allowing for vector and axial-vector couplings of a new Z' state to nucleons. The Z' has a mass of $O(10)$ MeV and emerges from the spontaneous breaking of the new gauge group, allowing it to be a possible explanation of the $X17$ anomaly. However, in order to comply with experimental bounds on flavour-violation in the quark sector, we have imposed that the first two quark generations are flavour-universal under this $U(1)'$ gauge group while the corresponding charges of the lepton sector are left as fully non-universal. As a consequence, couplings of the Z' state with all light neutrinos are present in the model and may manifest themselves in NSIs of neutrinos affecting neutrino flavour ratios in matter.

We have constrained this theoretical construction with data from the ATOMKI collaboration and other low energy experiments, such as NA64 searches for Z' , data on $(g-2)_{e,\mu}$,

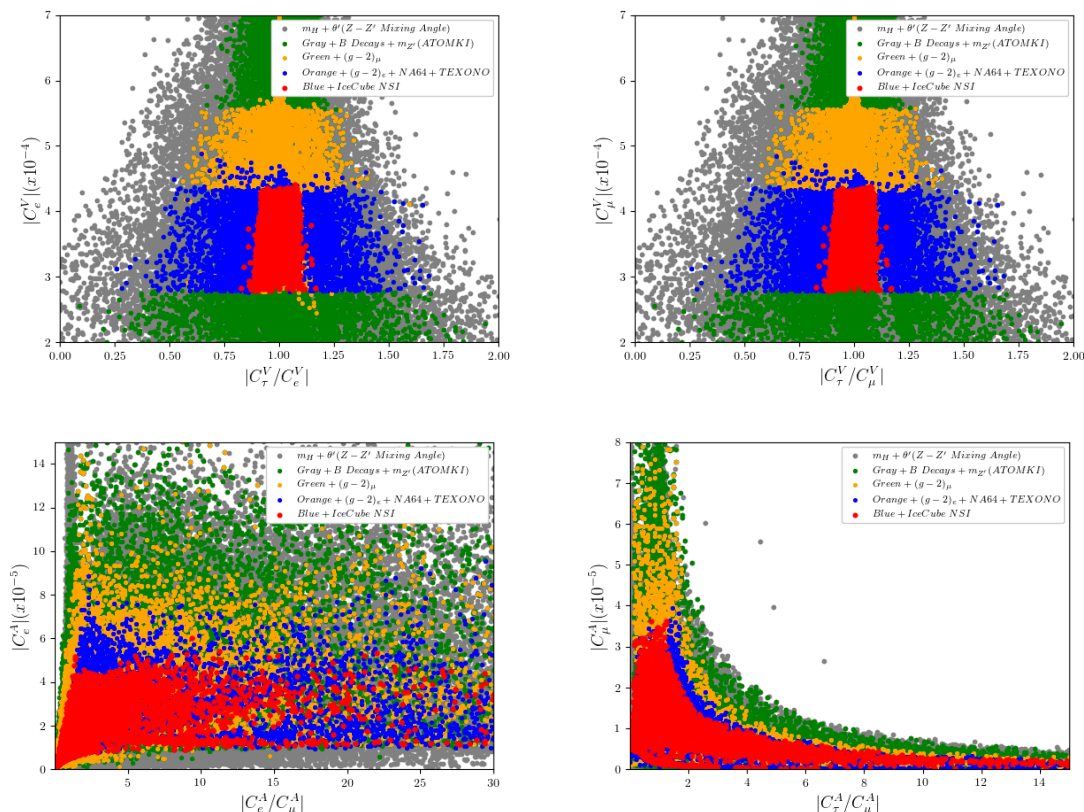


Figure 4. The allowed regions for the ratios of Z' vector (top) and axial-vector (bottom) couplings with e, μ and τ leptons. Here, the colour convention is the same as in figure 2.

constraints from CEvNS, Moller scattering and atomic parity violation, and finally with NSI data from the IceCube neutrino experiment (complementing earlier data from TEXONO).

IceCube data constrain the vector parts of the Z' interactions with leptons to be nearly flavour-universal while they give no constraints on the universality of the axial vector part. In the neutrino sector the constraints on $\mu - \tau$ universality are strong while $e - \mu$ universality is somewhat less constrained by the IceCube results. The results also exclude a scenario where the Z' couples only to electrons. This means that almost flavour-universal couplings with charged leptons are possible, facilitating searches in leptonic channels at colliders and low-energy experiments.

We have in the end found that there are sizeable regions of parameter space in this theoretical framework that can accommodate all such constraints. We have also defined four benchmark points that can be used in further phenomenological investigation of the model described.

Acknowledgments

SM is supported in part through the NExT Institute and the STFC Consolidated Grant No. ST/L000296/1. The work of YH is supported by Balikesir University Scientific Research Projects with Grant No. BAP-2022/083. YH thanks the other authors for their hospitality

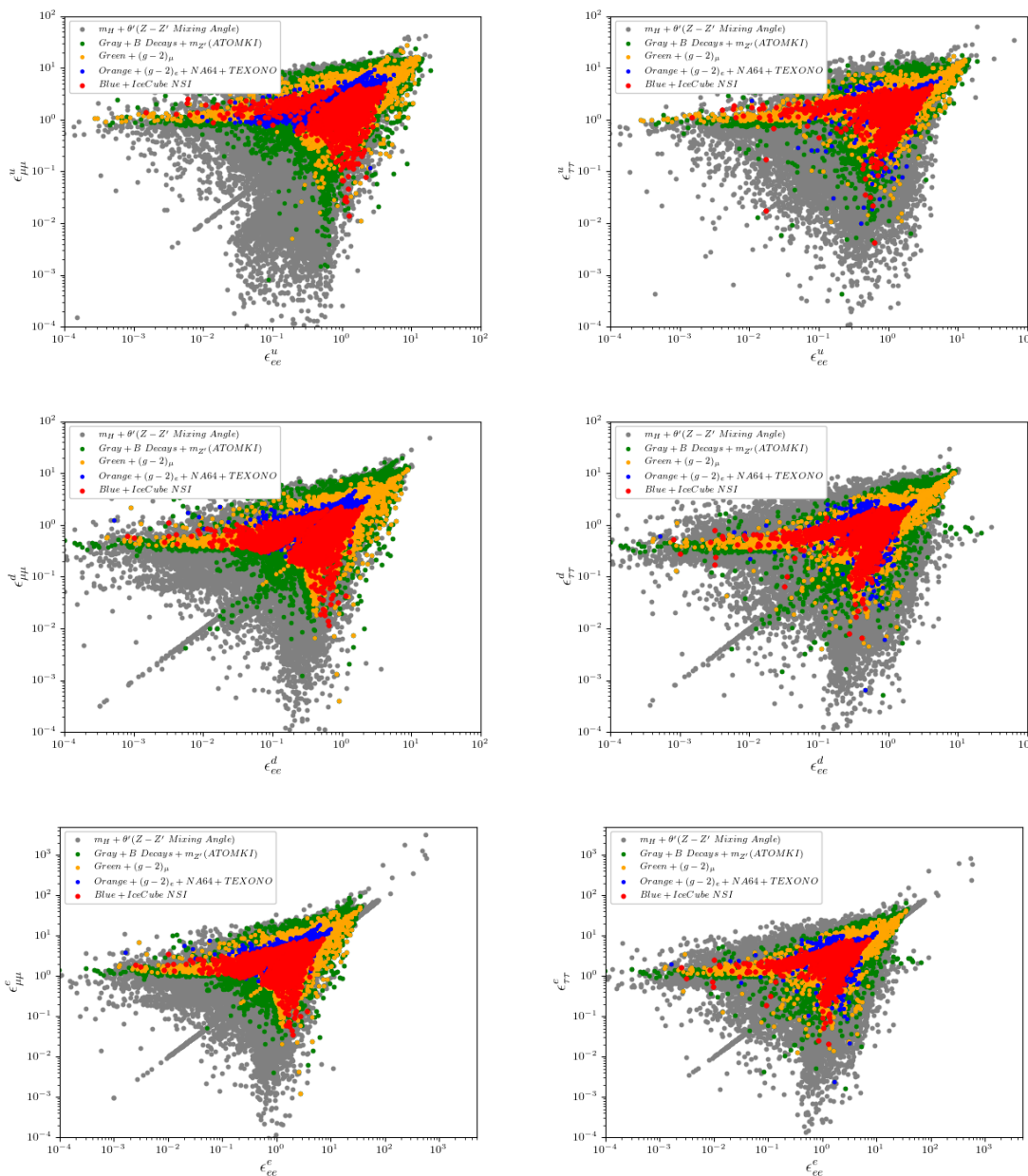


Figure 5. The allowed regions for NSI effective couplings of neutrinos with up-quarks (top), down-quarks (middle) and electrons (bottom) via Z' mediation. The colour convention is the same as in figure 2.

during a visit to Uppsala, which initiated this work, under the auspices of the Erasmus+ Staff Mobility for Training. CPH is supported by grant no. 2021-04759 from the Swedish Research Council. HW is supported by the Carl Trygger Foundation under grant no. CTS18:164 and the Ruth and Nils-Erik Stenbäcks Foundation.

Parameters	BP1	BP2	BP3	BP4
g'	1.16×10^{-5}	1.45×10^{-5}	2.31×10^{-5}	1.20×10^{-5}
\tilde{g}	-4.97×10^{-4}	-4.69×10^{-4}	-5.10×10^{-4}	-5.32×10^{-4}
v'	746	588	369	691
λ_χ	0.007	0.003	0.006	0.009
κ	0.0079	0.0123	0.0087	0.0021
(m_{H_1}, m_{H_2})	(87.46, 124.34)	(45.30, 124.29)	(40.66, 125.35)	(93.86, 125.98)
$m_{Z'}$	0.0173	0.0172	0.0171	0.0166
(C_u^V, C_u^A)	$(-2.45 \times 10^{-4}, 1.41 \times 10^{-5})$	$(-2.51 \times 10^{-4}, -1.35 \times 10^{-5})$	$(-2.67 \times 10^{-4}, -1.12 \times 10^{-5})$	$(-2.78 \times 10^{-4}, -1.17 \times 10^{-5})$
(C_d^V, C_d^A)	$(1.29 \times 10^{-4}, -1.41 \times 10^{-5})$	$(1.18 \times 10^{-4}, 1.34 \times 10^{-5})$	$(1.27 \times 10^{-4}, 1.12 \times 10^{-5})$	$(1.33 \times 10^{-4}, 1.17 \times 10^{-5})$
(C_e^V, C_e^A)	$(3.61 \times 10^{-4}, 0)$	$(3.83 \times 10^{-4}, 0)$	$(4.06 \times 10^{-4}, 0)$	$(4.23 \times 10^{-4}, 0)$
(C_{ν_e}, C_{ν_μ})	$(-1.47 \times 10^{-5}, -1.36 \times 10^{-5})$	$(1.42 \times 10^{-5}, 1.27 \times 10^{-5})$	$(1.01 \times 10^{-5}, 1.23 \times 10^{-5})$	$(1.05 \times 10^{-5}, 1.29 \times 10^{-5})$
$(\epsilon_{ee}^u, \epsilon_{\mu\mu}^u, \epsilon_{\tau\tau}^u)$	(1.45, 1.33, 1.05)	(-1.46, -1.31, -0.94)	(-1.11, -1.37, -2.01)	(-1.27, -1.56, -2.29)
$(\epsilon_{ee}^d, \epsilon_{\mu\mu}^d, \epsilon_{\tau\tau}^d)$	(-0.76, -0.71, -0.55)	(0.69, 0.62, 0.44)	(0.53, 0.65, 0.96)	(0.61, 0.75, 1.10)
$(\epsilon_{ee}^e, \epsilon_{\mu\mu}^e, \epsilon_{\tau\tau}^e)$	(-2.13, -1.96, -1.54)	(2.24, 2.01, 1.43)	(1.69, 2.08, 3.06)	(1.93, 2.38, 3.49)
$\epsilon_{ee}^{\oplus} - \epsilon_{\mu\mu}^{\oplus}$	-0.007	-0.008	0.013	0.011
$\epsilon_{\tau\tau}^{\oplus} - \epsilon_{\mu\mu}^{\oplus}$	0.017	0.021	-0.028	-0.032
Q'_{u_1}	2.0	-1.2	-0.4	-0.8
Q'_{u_2}	2.0	-1.2	-0.4	-0.8
Q'_{u_3}	1.6	-0.8	-0.8	-1.61
Q'_{d_1}	-1.0	0.6	0.2	0.4
Q'_{d_2}	-1.0	0.6	0.2	0.4
Q'_{d_3}	-1.0	0.6	0.2	0.4
Q'_{Q_1}	0.5	-0.3	-0.1	-0.2
Q'_{Q_2}	0.5	-0.3	-0.1	-0.2
Q'_{Q_3}	0.3	-0.1	-0.3	-0.6
Q'_{e_1}	-2.9	1.7	0.7	1.4
Q'_{e_2}	-3.1	1.9	0.5	1.0
Q'_{e_3}	-2.2	1.0	1.4	2.8
Q'_{L_1}	-1.6	1.0	0.2	0.4
Q'_{L_2}	-1.4	0.8	0.4	0.8
Q'_{L_3}	-0.9	0.3	0.9	1.8
Q'_{ν_1}	0	0	0	0
Q'_{ν_2}	0	0	0	0
Q'_{ν_3}	-0.4	0.4	-0.4	-0.8
Q'_H	1.3	-0.7	-0.5	-1

Table 3. The BPs which are selected to be consistent with all experimental constraints as well as NSI results from IceCube. All masses are given in GeV.

Data Availability Statement. This article has no associated data or the data will not be deposited.

Code Availability Statement. This article has no associated code or the code will not be deposited.

Open Access. This article is distributed under the terms of the Creative Commons Attribution License ([CC-BY4.0](https://creativecommons.org/licenses/by/4.0/)), which permits any use, distribution and reproduction in any medium, provided the original author(s) and source are credited.

References

- [1] CMS collaboration, *Observation of a New Boson at a Mass of 125 GeV with the CMS Experiment at the LHC*, *Phys. Lett. B* **716** (2012) 30 [[arXiv:1207.7235](https://arxiv.org/abs/1207.7235)] [[INSPIRE](#)].
- [2] ATLAS collaboration, *Observation of a new particle in the search for the Standard Model Higgs boson with the ATLAS detector at the LHC*, *Phys. Lett. B* **716** (2012) 1 [[arXiv:1207.7214](https://arxiv.org/abs/1207.7214)] [[INSPIRE](#)].
- [3] MUON G-2 collaboration, *Final Report of the Muon E821 Anomalous Magnetic Moment Measurement at BNL*, *Phys. Rev. D* **73** (2006) 072003 [[hep-ex/0602035](https://arxiv.org/abs/hep-ex/0602035)] [[INSPIRE](#)].
- [4] A.J. Krasznahorkay et al., *Observation of Anomalous Internal Pair Creation in Be8: A Possible Indication of a Light, Neutral Boson*, *Phys. Rev. Lett.* **116** (2016) 042501 [[arXiv:1504.01527](https://arxiv.org/abs/1504.01527)] [[INSPIRE](#)].
- [5] D.S.M. Alves et al., *Shedding light on X17: community report*, *Eur. Phys. J. C* **83** (2023) 230 [[INSPIRE](#)].
- [6] X. Zhang and G.A. Miller, *Can nuclear physics explain the anomaly observed in the internal pair production in the Beryllium-8 nucleus?*, *Phys. Lett. B* **773** (2017) 159 [[arXiv:1703.04588](https://arxiv.org/abs/1703.04588)] [[INSPIRE](#)].
- [7] B. Koch, *X17: A new force, or evidence for a hard $\gamma + \gamma$ process?*, *Nucl. Phys. A* **1008** (2021) 122143 [[arXiv:2003.05722](https://arxiv.org/abs/2003.05722)] [[INSPIRE](#)].
- [8] A.C. Hayes, J.L. Friar, G.M. Hale and G.T. Garvey, *Angular correlations in the e^+e^- decay of excited states in Be8*, *Phys. Rev. C* **105** (2022) 055502 [[arXiv:2106.06834](https://arxiv.org/abs/2106.06834)] [[INSPIRE](#)].
- [9] M. Viviani et al., *X17 boson and the ${}^3\text{H}(p, e^+e^-){}^4\text{He}$ and ${}^3\text{He}(n, e^+e^-){}^4\text{He}$ processes: A theoretical analysis*, *Phys. Rev. C* **105** (2022) 014001 [[arXiv:2104.07808](https://arxiv.org/abs/2104.07808)] [[INSPIRE](#)].
- [10] J.L. Feng et al., *Protophobic Fifth-Force Interpretation of the Observed Anomaly in ${}^8\text{Be}$ Nuclear Transitions*, *Phys. Rev. Lett.* **117** (2016) 071803 [[arXiv:1604.07411](https://arxiv.org/abs/1604.07411)] [[INSPIRE](#)].
- [11] J.L. Feng et al., *Particle physics models for the 17 MeV anomaly in beryllium nuclear decays*, *Phys. Rev. D* **95** (2017) 035017 [[arXiv:1608.03591](https://arxiv.org/abs/1608.03591)] [[INSPIRE](#)].
- [12] J.L. Feng, T.M.P. Tait and C.B. Verhaaren, *Dynamical Evidence For a Fifth Force Explanation of the ATOMKI Nuclear Anomalies*, *Phys. Rev. D* **102** (2020) 036016 [[arXiv:2006.01151](https://arxiv.org/abs/2006.01151)] [[INSPIRE](#)].
- [13] T. Nomura and P. Sanyal, *Explaining Atomki anomaly and muon $g - 2$ in $U(1)_X$ extended flavour violating two Higgs doublet model*, *JHEP* **05** (2021) 232 [[arXiv:2010.04266](https://arxiv.org/abs/2010.04266)] [[INSPIRE](#)].
- [14] O. Seto and T. Shimomura, *Atomki anomaly in gauged $U(1)_R$ symmetric model*, *JHEP* **04** (2021) 025 [[arXiv:2006.05497](https://arxiv.org/abs/2006.05497)] [[INSPIRE](#)].

- [15] J. Kozaczuk, D.E. Morrissey and S.R. Stroberg, *Light axial vector bosons, nuclear transitions, and the ^8Be anomaly*, *Phys. Rev. D* **95** (2017) 115024 [[arXiv:1612.01525](#)] [[INSPIRE](#)].
- [16] L. Delle Rose, S. Khalil, S.J.D. King and S. Moretti, *New Physics Suggested by Atomki Anomaly*, *Front. in Phys.* **7** (2019) 73 [[arXiv:1812.05497](#)] [[INSPIRE](#)].
- [17] C.H. Nam, *17 MeV Atomki anomaly from short-distance structure of spacetime*, *Eur. Phys. J. C* **80** (2020) 231 [[arXiv:1907.09819](#)] [[INSPIRE](#)].
- [18] X. Zhang and G.A. Miller, *Can a protophobic vector boson explain the ATOMKI anomaly?*, *Phys. Lett. B* **813** (2021) 136061 [[arXiv:2008.11288](#)] [[INSPIRE](#)].
- [19] D. Barducci and C. Toni, *An updated view on the ATOMKI nuclear anomalies*, *JHEP* **02** (2023) 154 [*Erratum ibid.* **07** (2023) 168] [[arXiv:2212.06453](#)] [[INSPIRE](#)].
- [20] P.B. Denton and J. Gehrlein, *Neutrino constraints and the ATOMKI X17 anomaly*, *Phys. Rev. D* **108** (2023) 015009 [[arXiv:2304.09877](#)] [[INSPIRE](#)].
- [21] NA48/2 collaboration, *Search for the dark photon in π^0 decays*, *Phys. Lett. B* **746** (2015) 178 [[arXiv:1504.00607](#)] [[INSPIRE](#)].
- [22] M. Hostert and M. Pospelov, *Pion decay constraints on exotic 17 MeV vector bosons*, *Phys. Rev. D* **108** (2023) 055011 [[arXiv:2306.15077](#)] [[INSPIRE](#)].
- [23] SINDRUM collaboration, *Measurement of the Decay $\pi^+ \rightarrow e^+ \nu_e e^+ e^-$ and Search for a Light Higgs Boson*, *Phys. Lett. B* **222** (1989) 533 [[INSPIRE](#)].
- [24] B. Pulice, *A Family-nonuniversal $U(1)'$ Model for Excited Beryllium Decays*, *Chin. J. Phys.* **71** (2021) 506 [[arXiv:1911.10482](#)] [[INSPIRE](#)].
- [25] L. Delle Rose et al., *Atomki Anomaly in Family-Dependent $U(1)'$ Extension of the Standard Model*, *Phys. Rev. D* **99** (2019) 055022 [[arXiv:1811.07953](#)] [[INSPIRE](#)].
- [26] P.S. Bhupal Dev et al., *Neutrino Non-Standard Interactions: A Status Report*, *SciPost Phys. Proc.* **2** (2019) 001 [[arXiv:1907.00991](#)] [[INSPIRE](#)].
- [27] TEXONO collaboration, *Measurement of $\bar{\nu}_e$ -Electron Scattering Cross-Section with a CsI(Tl) Scintillating Crystal Array at the Kuo-Sheng Nuclear Power Reactor*, *Phys. Rev. D* **81** (2010) 072001 [[arXiv:0911.1597](#)] [[INSPIRE](#)].
- [28] S. Bilmis et al., *Constraints on Dark Photon from Neutrino-Electron Scattering Experiments*, *Phys. Rev. D* **92** (2015) 033009 [[arXiv:1502.07763](#)] [[INSPIRE](#)].
- [29] J.M. Cabarcas, A. Parada and N. Quintero-Poveda, *Implications of NSI constraints from ANTARES and IceCube on a simplified Z' model*, *Phys. Lett. B* **848** (2024) 138339 [[arXiv:2304.01388](#)] [[INSPIRE](#)].
- [30] ICECUBE collaboration, *All-flavor constraints on nonstandard neutrino interactions and generalized matter potential with three years of IceCube DeepCore data*, *Phys. Rev. D* **104** (2021) 072006 [[arXiv:2106.07755](#)] [[INSPIRE](#)].
- [31] C. Coriano, L. Delle Rose and C. Marzo, *Constraints on abelian extensions of the Standard Model from two-loop vacuum stability and $U(1)_{B-L}$* , *JHEP* **02** (2016) 135 [[arXiv:1510.02379](#)] [[INSPIRE](#)].
- [32] Y. Hiçyılmaz, S. Khalil and S. Moretti, *Light Z' signatures at the LHC*, *Phys. Rev. D* **107** (2023) 035030 [[arXiv:2209.09226](#)] [[INSPIRE](#)].
- [33] DELPHI collaboration, *A study of radiative muon pair events at Z^0 energies and limits on an additional Z' gauge boson*, *Z. Phys. C* **65** (1995) 603 [[INSPIRE](#)].

- [34] J. Erler, P. Langacker, S. Munir and E. Rojas, *Improved Constraints on Z-prime Bosons from Electroweak Precision Data*, *JHEP* **08** (2009) 017 [[arXiv:0906.2435](#)] [[INSPIRE](#)].
- [35] J.P. Leveille, *The Second Order Weak Correction to $(G-2)$ of the Muon in Arbitrary Gauge Models*, *Nucl. Phys. B* **137** (1978) 63 [[INSPIRE](#)].
- [36] A. Bodas, R. Coy and S.J.D. King, *Solving the electron and muon $g - 2$ anomalies in Z' models*, *Eur. Phys. J. C* **81** (2021) 1065 [[arXiv:2102.07781](#)] [[INSPIRE](#)].
- [37] C. Bobeth et al., *$B_{s,d} \rightarrow l^+l^-$ in the Standard Model with Reduced Theoretical Uncertainty*, *Phys. Rev. Lett.* **112** (2014) 101801 [[arXiv:1311.0903](#)] [[INSPIRE](#)].
- [38] A.J. Buras, F. De Fazio, J. Girrbach and M.V. Carlucci, *The Anatomy of Quark Flavour Observables in 331 Models in the Flavour Precision Era*, *JHEP* **02** (2013) 023 [[arXiv:1211.1237](#)] [[INSPIRE](#)].
- [39] M. Lindner, F.S. Queiroz, W. Rodejohann and X.-J. Xu, *Neutrino-electron scattering: general constraints on Z' and dark photon models*, *JHEP* **05** (2018) 098 [[arXiv:1803.00060](#)] [[INSPIRE](#)].
- [40] Y. Grossman, *Nonstandard neutrino interactions and neutrino oscillation experiments*, *Phys. Lett. B* **359** (1995) 141 [[hep-ph/9507344](#)] [[INSPIRE](#)].
- [41] T. Ohlsson, *Status of non-standard neutrino interactions*, *Rept. Prog. Phys.* **76** (2013) 044201 [[arXiv:1209.2710](#)] [[INSPIRE](#)].
- [42] L. Wolfenstein, *Neutrino Oscillations in Matter*, *Phys. Rev. D* **17** (1978) 2369 [[INSPIRE](#)].
- [43] S.P. Mikheyev and A.Y. Smirnov, *Resonance Amplification of Oscillations in Matter and Spectroscopy of Solar Neutrinos*, *Sov. J. Nucl. Phys.* **42** (1985) 913 [[INSPIRE](#)].
- [44] A. Serenelli, S. Basu, J.W. Ferguson and M. Asplund, *New Solar Composition: The Problem With Solar Models Revisited*, *Astrophys. J. Lett.* **705** (2009) L123 [[arXiv:0909.2668](#)] [[INSPIRE](#)].
- [45] E. Lisi and D. Montanino, *Earth regeneration effect in solar neutrino oscillations: An analytic approach*, *Phys. Rev. D* **56** (1997) 1792 [[hep-ph/9702343](#)] [[INSPIRE](#)].
- [46] I. Esteban et al., *Updated constraints on non-standard interactions from global analysis of oscillation data*, *JHEP* **08** (2018) 180 [Addendum *ibid.* **12** (2020) 152] [[arXiv:1805.04530](#)] [[INSPIRE](#)].
- [47] W. Porod, *SPheno, a program for calculating supersymmetric spectra, SUSY particle decays and SUSY particle production at e^+e^- colliders*, *Comput. Phys. Commun.* **153** (2003) 275 [[hep-ph/0301101](#)] [[INSPIRE](#)].
- [48] W. Porod and F. Staub, *SPheno 3.1: Extensions including flavour, CP-phases and models beyond the MSSM*, *Comput. Phys. Commun.* **183** (2012) 2458 [[arXiv:1104.1573](#)] [[INSPIRE](#)].
- [49] J. Braathen, M.D. Goodsell and F. Staub, *Supersymmetric and non-supersymmetric models without catastrophic Goldstone bosons*, *Eur. Phys. J. C* **77** (2017) 757 [[arXiv:1706.05372](#)] [[INSPIRE](#)].
- [50] F. Staub, *SARAH 4: A tool for (not only SUSY) model builders*, *Comput. Phys. Commun.* **185** (2014) 1773 [[arXiv:1309.7223](#)] [[INSPIRE](#)].
- [51] F. Staub, *Exploring new models in all detail with SARAH*, *Adv. High Energy Phys.* **2015** (2015) 840780 [[arXiv:1503.04200](#)] [[INSPIRE](#)].
- [52] HFLAV collaboration, *Averages of B-Hadron, C-Hadron, and τ -Lepton Properties as of early 2012*, [arXiv:1207.1158](#) [[INSPIRE](#)].

- [53] LHCb collaboration, *First Evidence for the Decay $B_s^0 \rightarrow \mu^+ \mu^-$* , *Phys. Rev. Lett.* **110** (2013) 021801 [[arXiv:1211.2674](#)] [[INSPIRE](#)].
- [54] HFLAV collaboration, *Averages of b -hadron, c -hadron, and τ -lepton properties*, [arXiv:1010.1589](#) [[INSPIRE](#)].
- [55] MUON G-2 collaboration, *Measurement of the Positive Muon Anomalous Magnetic Moment to 0.20 ppm*, *Phys. Rev. Lett.* **131** (2023) 161802 [[arXiv:2308.06230](#)] [[INSPIRE](#)].
- [56] L. Morel, Z. Yao, P. Cladé and S. Guellati-Khélifa, *Determination of the fine-structure constant with an accuracy of 81 parts per trillion*, *Nature* **588** (2020) 61 [[INSPIRE](#)].
- [57] NA64 collaboration, *Improved limits on a hypothetical $X(16.7)$ boson and a dark photon decaying into e^+e^- pairs*, *Phys. Rev. D* **101** (2020) 071101 [[arXiv:1912.11389](#)] [[INSPIRE](#)].
- [58] SLAC E158 collaboration, *Precision measurement of the weak mixing angle in Moller scattering*, *Phys. Rev. Lett.* **95** (2005) 081601 [[hep-ex/0504049](#)] [[INSPIRE](#)].
- [59] Y. Kahn, G. Krnjaic, S. Mishra-Sharma and T.M.P. Tait, *Light Weakly Coupled Axial Forces: Models, Constraints, and Projections*, *JHEP* **05** (2017) 002 [[arXiv:1609.09072](#)] [[INSPIRE](#)].
- [60] S.G. Porsev, K. Beloy and A. Derevianko, *Precision determination of electroweak coupling from atomic parity violation and implications for particle physics*, *Phys. Rev. Lett.* **102** (2009) 181601 [[arXiv:0902.0335](#)] [[INSPIRE](#)].
- [61] G. Arcadi, M. Lindner, J. Martins and F.S. Queiroz, *New physics probes: Atomic parity violation, polarized electron scattering and neutrino-nucleus coherent scattering*, *Nucl. Phys. B* **959** (2020) 115158 [[arXiv:1906.04755](#)] [[INSPIRE](#)].
- [62] D. Aristizabal Sierra, V. De Romeri and D.K. Papoulias, *Consequences of the Dresden-II reactor data for the weak mixing angle and new physics*, *JHEP* **09** (2022) 076 [[arXiv:2203.02414](#)] [[INSPIRE](#)].
- [63] M. Atzori Corona et al., *Probing light mediators and $(g-2)_\mu$ through detection of coherent elastic neutrino nucleus scattering at COHERENT*, *JHEP* **05** (2022) 109 [[arXiv:2202.11002](#)] [[INSPIRE](#)].
- [64] P. Coloma et al., *Bounds on new physics with data of the Dresden-II reactor experiment and COHERENT*, *JHEP* **05** (2022) 037 [[arXiv:2202.10829](#)] [[INSPIRE](#)].